

# The Larger Grain and (111)-Orientation Planes of Poly-Ge Thin Film Grown on SiO<sub>2</sub> Substrate by Al-Induced Crystallization

Shaoguang Dong, Junhuo Zhuang, Yaguang Zeng

Physics and Illumination Department of Foshan University, Foshan, China  
Email: dshgfosu@126.com

**How to cite this paper:** Dong, S.G., Zhuang, J.H. and Zeng, Y.G. (2018) The Larger Grain and (111)-Orientation Planes of Poly-Ge Thin Film Grown on SiO<sub>2</sub> Substrate by Al-Induced Crystallization. *Journal of Materials Science and Chemical Engineering*, 6, 22-32.

<https://doi.org/10.4236/msce.2018.62003>

**Received:** April 23, 2017

**Accepted:** February 10, 2018

**Published:** February 13, 2018

Copyright © 2018 by authors and Scientific Research Publishing Inc.  
This work is licensed under the Creative Commons Attribution International License (CC BY 4.0).

<http://creativecommons.org/licenses/by/4.0/>



Open Access

## Abstract

Al-induced crystallization yields the larger grain and (111)-orientation planes of poly-Ge thin film grown on SiO<sub>2</sub> substrate, the (111)-orientation planes of poly-Ge thin film grown on SiO<sub>2</sub> substrate are very important for the superior performance electronics and solar cells. We discussed the 50 nm thickness poly-Ge thin film grown on SiO<sub>2</sub> substrate by Al-induced crystallization focusing on the lower annealing temperature and the diffusion control interlayer between Ge and Al thin film. The (111)-orientation planes ratio of poly-Ge thin film achieve as high as 90% by merging the lower annealing temperature (325°C) and the GeO<sub>x</sub> diffusion control interlayer. Moreover, we find the lack of defects on poly-Ge thin film surface and the larger average grains size of poly-Ge thin film over 12 μm were demonstrated by electron backscatter diffraction measurement. Our results turn on the feasibility of fabricating electronic and optical device with poly-Ge thin film grown on SiO<sub>2</sub> substrate.

## Keywords

Al-Induced Crystallization, Poly-Ge Thin Film, Diffusion Control Interlayer, Lower Annealing Temperature

## 1. Introduction

The high quality poly-Ge thin film has many applications, for example, thin film transistors and highly conversion efficiency solar cells [1]. A larger grain and (111)-orientation planes ratio of poly-Ge thin film is specifically desirable because it is very suitable for acting as the epitaxial template for III-V group semiconductors materials [2]. In particular, the (111)-orientation planes of poly-Ge thin film can provide the highest carrier mobility and treated as the epitaxial

template, which require lower growing temperature ( $<400^{\circ}\text{C}$  for integrated circuits,  $<550^{\circ}\text{C}$  for glass substrates) [3]. Hence, fabricating such poly-Ge thin film on  $\text{SiO}_2$  substrate may develop novel devices with advanced function. But Ge-based flexible devices desire lower temperature growth technique of high quality poly-Ge thin film grown on  $\text{SiO}_2$  substrate. Al-induced crystallization is one of the metal induced solid phase crystallization techniques for a-Si thin film grown on  $\text{SiO}_2$  substrate, in order to form the larger grain poly-Si thin film at lower growing temperature ( $420^{\circ}\text{C}$  -  $550^{\circ}\text{C}$ ) through the layer exchange between Al and Si thin film [4]. Recently, the preferentially (111)-orientation planes poly-Ge thin film with the larger grain can be achieved through the layer exchange between Ge and Al thin film during Al-induced crystallization [5]. Moreover, K. Toko *et al.* have improved the (111)-orientation planes ratio and the average grains size of poly-Ge thin film significantly by forming the diffusion control interlayer ( $\text{AlO}_x$ ) between Ge and Al thin film during Al-induced crystallization [1]. However, it is still difficult to achieve the larger grain poly-Ge thin film on  $\text{SiO}_2$  substrate below the softening substrate temperature ( $<200^{\circ}\text{C}$ ).

M. Kurosawa *et al.* recently studied Al-induced crystallization of the a-Ge thin film on  $\text{SiO}_2$  substrate, and they have acquired the preferentially (111)-orientation planes ( $\sim 68\%$ ) poly-Ge thin film by decreasing the thickness of Al and Ge thin film to 50 nm [6]. Hu *et al.* have achieved the (111)-orientation planes poly-Ge ( $\sim 70\%$ ) thin film on  $\text{SiO}_2$  substrate by using the  $\text{GeO}_x$  diffusion control interlayer structure during Al-induced crystallization [7]. From Al-induced crystallization of the a-Ge thin film in our first experiments, we have gained (111)-orientation planes ( $\sim 90\%$ ) poly-Ge thin film grown on  $\text{SiO}_2$  substrate by lowering the annealing temperature to  $325^{\circ}\text{C}$  and forming  $\text{AlO}_x$  diffusion control interlayer at the same time. In our second experiments, we investigate Al-induced crystallization of the poly-Ge thin film by lowering the crystallization temperature, which is depended on the layer exchange growth mechanism. The larger grains and (111)-orientation planes poly-Ge thin film on  $\text{SiO}_2$  substrate can be achieved by Al-induced crystallization technique at temperatures as low as  $180^{\circ}\text{C}$ . We can also control the crystal orientation of poly-Ge thin film to (111)-orientation planes by regulating the annealing temperature during Al-induced crystallization, or the thickness of Al and Si thin film and the diffusion control interlayer ( $\text{AlO}_x$  or  $\text{GeO}_x$ ) between Si and Al thin film [8].

## 2. Experimental Details

During our first experiment, all Al thin films were deposited on  $\text{SiO}_2$  substrate at first, Al thin films were exposed to air for 1 min, 5 min and 30 min ( $t_{\text{air}}$ ) to grow native  $\text{AlO}_x$  thin film as the diffusion control interlayer subsequently. Because the different exposure times corresponding to the different thicknesses of  $\text{AlO}_x$  thin film. Afterwards, all a-Ge thin films were grown on these  $\text{AlO}_x$  thin films. The thickness of Al and a-Ge thin film was measured to be 50 nm, this thickness size is advantageous for the optimize (111)-orientation planes [5]. All thin films

were grown by using a RF magnetron sputtering method at room temperature. Finally, these thin films were annealed in  $N_2$  at the annealing temperature ( $T_a$ ) 325°C, 350°C, 375°C for 10 - 400 h. Because the annealing temperature should impact the (111)-orientation planes ratio of the poly-Ge thin film. These thin films preparation procedure is schematically shown in **Figure 1**. During Al-induced crystallization, the surface morphology of crystallized poly-Ge thin film was estimated by Normarki optical microscopy, Ge and Al elemental composition in crystallized poly-Ge thin film were evaluated by energy dispersive X-ray (EDX) analysis, the crystal state of crystallized poly-Ge thin film was appraised by X-ray diffraction (XRD) measurement, the (111)-orientation planes of crystallized poly-Ge thin film was observed by electron backscattered diffraction (EBSD) measurement. Before EBSD measurement, these Al thin films and  $AlO_x$  diffusion control interlayers on poly-Ge thin film were removed by HF solutions (~1.5%).

In our second experiments, four kinds of thin film were prepared and summarized in **Table 1**. Thin film A was grown as follows: 50 nm thickness Al thin film was grown on  $SiO_2$  substrate, and bared to air for 5 min to get the native  $AlO_x$  diffusion control interlayer, followed by a 50 nm thickness a-Ge thin film preparation. Thin film B has the same stacked layer structure as thin film A except that it additionally has 1 nm thickness a-Ge insertion interlayer below Al thin film or on  $SiO_2$  substrate. Thin film C has the native  $GeO_x$  diffusion control interlayer in substitution for the  $AlO_x$  diffusion control interlayer in thin film A. Here, the  $GeO_x$  diffusion control interlayer was prepared by 1 nm thickness a-Ge thin film grown on Al thin film which is exposed to air for 24 h. Thin film D has both of a-Ge insertion interlayer and  $GeO_x$  diffusion control interlayer. Al and Ge thin film were prepared at room temperature using a RF magnetron sputtering method. Finally, these thin films were annealed at 180°C - 350°C in  $N_2$  for 0.1 - 100 h to induce layer exchange. By removing Al thin film and  $AlO_x$  or  $GeO_x$  diffusion control interlayer using HF solutions (1.5%) for 1 min, exposed poly-Ge film was obtained on  $SiO_2$  substrate. The poly-Ge thin film preparation procedure is shown in **Figure 2** schematically. The crystallization time (the time for completing layer exchange in each thin film) was measured using Normarski optical microscopy and Raman scattering spectroscopy. The crystal

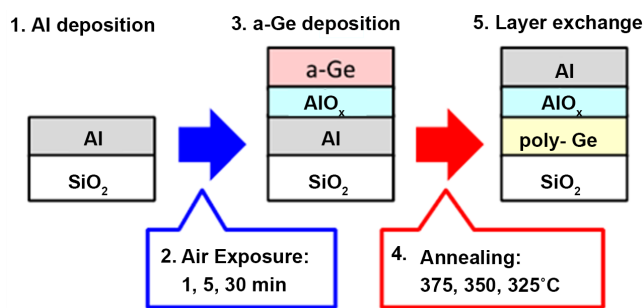


**Figure 1.** Schematic structure of poly-Ge thin film preparation procedure in our first experiments.

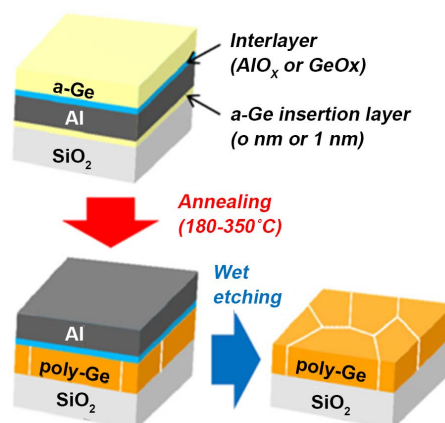


**Figure 2.** Schematic structures of the poly-Ge thin film preparation procedure in our second experiments.

**Table 1.** Poly-Ge thin film prepared in our second experiments.

Thin films	Interlayer between Ge and Al	Insertion layer
A	AlO <sub>x</sub>	None
B	AlO <sub>x</sub>	1-nm thickness a-Ge
C	GeO <sub>x</sub>	None
D	GeO <sub>x</sub>	1-nm thickness a-Ge

(111)-orientation planes of poly-Ge thin film was roughly evaluated by X-ray diffraction (XRD) rocking curve measurement. In addition, the detailed crystal (111)-orientation planes and the grain size were measured using electron back-scattered diffraction (EBSD) measurement.

### 3. Results and Discussions

The changes of a-Ge thin film with annealing time are revealed in **Figure 3** under  $t_{\text{air}} = 5$  min and  $T_{\text{a}} = 350^{\circ}\text{C}$  during Al-induced crystallization process. **Figure 3(a)-(c)** show the back surface of a-Ge thin film watched through the transparent SiO<sub>2</sub> substrate. Nomarski optical micrographs suggest that Ge atoms shift to the back surface of Al thin film by lateral growing, and finally cover the whole substrate during annealing time. **Figure 3(d)** and **Figure 3(e)** show EDX spectra achieved from a-Ge thin film surface before and after annealing time for 30 h, respectively. The voltage was 2.7 keV for the selective detection zone of elements near a-Ge thin film surface. These EDX spectra show that the surface thin film changed from Ge to Al during whole annealing time. **Figure 3(f)** shows the appearance of a sharp peak in XRD curve after annealing. The sharp peak near  $27^{\circ}$  relates to (111)-orientation planes of crystal Ge, and any other sharp peaks are not observed in the measured zone. These results show that Ge thin film crystallized and oriented to preferential (111)-orientation planes through layer exchange. The (111)-orientation planes ratio would be estimated precisely by EBSD measurement. We have affirmed a-Ge thin film has been accomplished on SiO<sub>2</sub> substrate through Al-induced crystallization process.

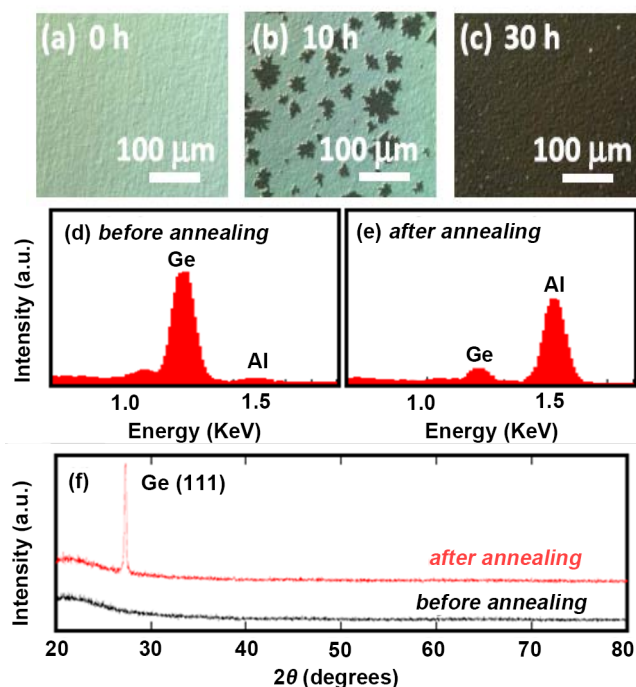


**Figure 3.** Ge atoms shift to the back surface (a), grow (b) and cover the whole substrate (c) during the annealing. These EDX spectra explain that the surface thin film changed from Ge to Al before (d) and after the whole annealing (e). The sharp peak near 27° appeared after annealing (f).

The EBSD measurement can characterize the (111)-orientation planes of poly-Ge thin film which depending on the  $T_a$  and  $t_{air}$  statistically during Al induced crystallization. The lower  $T_a$  and longer  $t_{air}$  demanded the longer annealing time to finish Al induced crystallization. Al induced crystallization of a-Si thin films had also the same tendency. [9] This tendency can be illustrated as follows: The lower  $T_a$  reduces the reaction rate of Al and Ge atoms by the Arrhenius law [10]; and the longer  $t_{air}$  thickens the  $AlO_x$  diffusion control interlayer, and decreases the diffusion rate of Al and Ge atoms [11]. The (111)-orientation planes of a-Ge thin film also depend on both  $T_a$  and  $t_{air}$  during Al induced crystallization, and the (111)-orientation planes become dominant with decreasing  $T_a$  and increasing  $t_{air}$ . This action is also the same as the a-Si thin film during Al induced crystallization [12]. The reason for this behavior can be explained as follows: The Ge nuclei happen on the surface of  $SiO_2$  substrate because the thickness of Ge and Al thin films is 50 nm [13], respectively, and (111)-orientation planes have the lowest interfacial energy in the diamond structure [14]. The lower  $T_a$  and longer  $t_{air}$  provide the lower reactive rate and lower diffusion rate of Ge and Al atoms. These reasons make it no chance to generate the other orientation planes with high interfacial energies, so resulting in the preferential (111)-orientation planes.

The EBSD measurement analysis results are shown in Figure 4. Here, the definition of the (111)-orientation planes ratio contain those planes which tilted

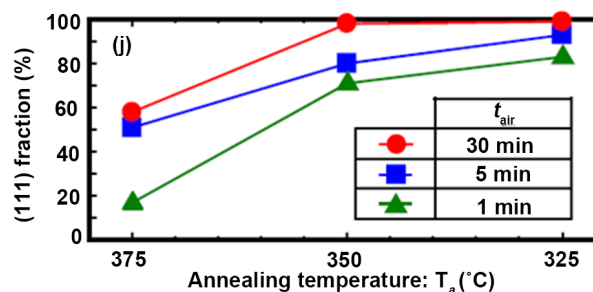


**Figure 4.** The (111)-orientation planes fraction reach over 90% by combining the lower  $T_a$  (325°C) and longer  $t_{air}$  (30 min).

within 10 from the exact (111)-orientation planes. **Figure 4** clearly shows that the (111)-orientation planes ratio increase with increasing  $t_{air}$  and decreasing  $T_a$ . We noticed that the (111)-orientation planes ratio reach over 90% by combining the lower  $T_a$  (325°C) and longer  $t_{air}$  (30 min). In the [15] report for Al induced crystallization of a-Ge thin film, the (111)-orientation planes fraction was limited to 68%. The main reason is the higher annealing temperature  $T_a$  (410°C). In addition, the EBSD measurement analysis found the average grain diameter is 12  $\mu\text{m}$  for these thin films. These grain diameter average values are the highest level in the previous reports about poly-Ge thin film on  $\text{SiO}_2$  substrates in lower annealing temperature process [16].

EDX analysis was also performed and the analysis results were shown in **Figure 5**. These data proved the layer exchange of Ge and Al thin film has been finished and the uniform formation of poly-Ge thin film on  $\text{SiO}_2$  substrate. The observed area did not contain any other kind of defects except (111)-orientation defects. Since (111)-orientation defects are related with the weakest bond in the diamond structure [17], and no other defects grown on the poly-Ge thin film surface. Consequently, Al induce crystallization of a-Ge thin film is useful as an epitaxial layer for those advanced flexible substrate materials.

In our second experiments, the thin films A, B, C, and D were annealed at 300°C, 275°C, 225°C, and 180°C, respectively. Nomarski optical microscopy suggested the completion of the layer exchange for all thin films after annealing time for 100 h. In addition, Raman spectra in **Figure 6(a)** show the largest sharp peak at around 292  $\text{cm}^{-1}$  for all thin films after annealing. These results indicate the crystallization of a-Ge thin film is better, although the sharp peak shift to the lower wave number compared to the crystal Ge actual sharp peak ( $\sim 300 \text{ cm}^{-1}$ ) [18]. These larger wave number shifts are not entirely understood, but they are possibly due to the residual Al atoms ( $\sim 0.5\%$ ) in Ge thin film. The insert figure in **Figure 6(a)** shows the full width at half maximum (FWHM) of Raman spectra sharp peak as a function of the annealing temperature. The FWHM is independent on the annealing temperature, whereas the FWHM increases with the annealing temperature decreasing for the solid phase crystallization of a-Ge thin films [19]. This result suggests that Al induced crystallization process is

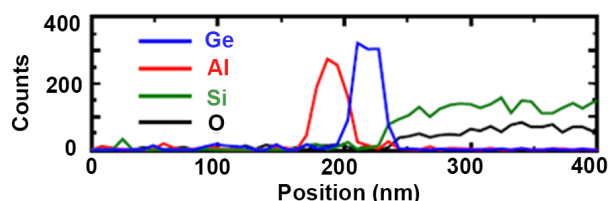


**Figure 5.** The layer exchange of Ge and Al thin film and the uniform formation of poly-Ge thin film on SiO<sub>2</sub> substrate.

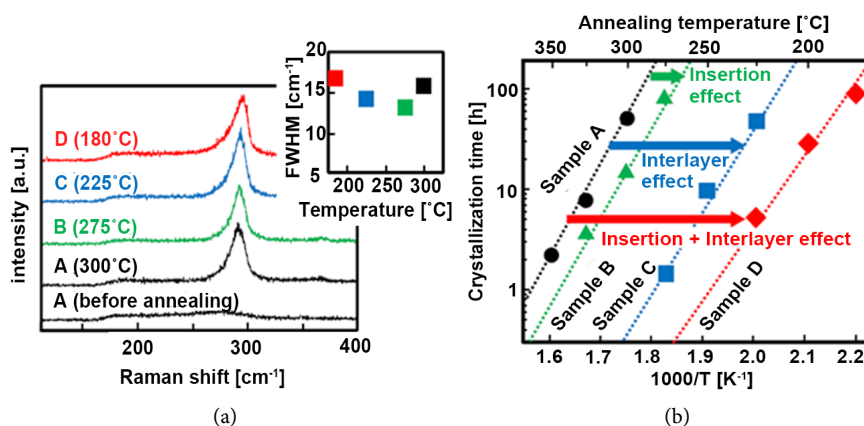


**Figure 6.** (a) Raman spectra for thin films A, B, C and D, where the annealing temperatures are 300°C for A, 275°C for B, 225°C for C, 180°C for D; (b) Arrhenius plots of the crystallization time for thin films A, B, C and D.

completely different from the solid phase crystallization process, Al induced crystallization proceeds through the a-Ge atoms diffusion and segregation in Al thin film[20].

**Figure 6(b)** shows the Arrhenius plots of the crystallization finish time for thin films A, B, C and D. Here, the crystallization finish time is defined as the time of the layer exchange completion. The resulting poly-Ge thin film region covers more than 95% area of SiO<sub>2</sub> substrate for all thin films. As seen in **Figure 6(b)**, the a-Ge insertion layer and the GeO<sub>x</sub> diffusion control interlayer work effectively for the lower crystallization temperature. In particular, thin film D, combining the a-Ge insertion layer and the GeO<sub>x</sub> diffusion control interlayer, significantly reduces the crystallization temperature to 180°C. The mechanism of the crystallization temperature reduction is explained as follows: during Al induced crystallization, Ge atoms diffuse from top a-Ge thin film to Al thin film through GeO<sub>x</sub> diffusion control interlayer. The Ge nucleation occurs when Ge atoms concentration in Al thin film is supersaturated. After that, the lateral growth of Ge crystals propagates due to the continuous supply of Ge atoms from top a-Ge thin film through GeO<sub>x</sub> the diffusion control interlayer. Based on these mechanisms, a-Ge insertion layer works for initial Ge atoms doped in Al thin film, which facilitates Ge atoms concentration supersaturation, but the GeO<sub>x</sub> diffusion control interlayer promotes Ge atoms diffusion compared to the conventional AlO<sub>x</sub> diffusion control interlayer.



The crystal (111)-orientation planes of poly-Ge for thin films A, B, C and D were characterized by the XRD rocking curve of (111)-orientation Ge reflection planes and summarized in **Figure 7**. All thin films have a sharp peak around  $13.7^\circ$  indicating preferential (111)-orientation planes. The (111)-orientation planes are interpreted from the viewpoint of the minimal interfacial energy between Ge thin film and  $\text{SiO}_2$  substrate [21]. The FWHM values of the sharp peak of XRD rocking curve are plotted in the insert figure, which indicates that the lower annealing temperature provides weaker (111)-orientation planes but larger FWHM values. This behavior is likely due to the unstable thermal equilibrium condition during the lower annealing temperature.

The crystal (111)-orientation planes and average the grain size of poly-Ge for thin films A, B, C and D were characterized using EBSD measurement. **Figures 8(a)-(d)** show the crystal (111)-orientation planes in the normal direction (ND). For the sample A, poly-Ge thin film has highly (111)-orientation planes. **Figure 8(e)-(h)** show the crystal other orientation plane in the transverse direction (TD) and indicate that the average grain size of poly-Ge thin film decrease with the annealing temperature decreasing. This result suggests that the a-Ge insertion layer and the  $\text{GeO}_x$  diffusion control interlayer increase the nucleation frequency and promote poly-Ge thin film crystallization. Nevertheless, **Figure 8(h)** indicates that the sample D has larger grain with approximately  $10\ \mu\text{m}$  even under the  $180^\circ\text{C}$  annealing temperature.

The (111)-orientation planes ratio and the average grain size of poly-Ge thin film were calculated using EBSD measurement. **Figure 9(a)** and **Figure 9(b)** show the typical (111)-orientation planes ratio and the average grain size of thin film D. **Figure 9(a)** indicates that poly-Ge thin film principally consists of planes with tilting within  $10^\circ$  of the exact (111)-orientation planes. This result agrees with XRD rocking curve in **Figure 7**. The whole (111)-orientation planes ratio was defined as the integrated values of the area ratios of exact (111)-orientation

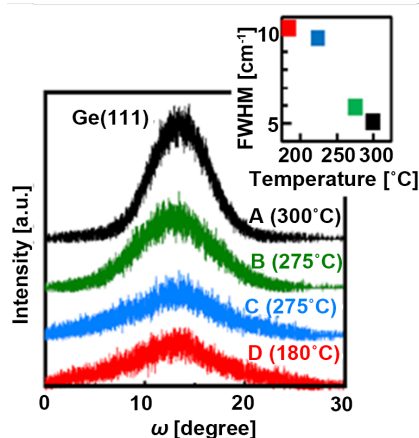


**Figure 7.** XRD rocking curves of (111)-orientation Ge reflection planes of thin films A, B, C and D. FWHM values for each thin film as a function of crystallization temperature are summarized in the insert figure.



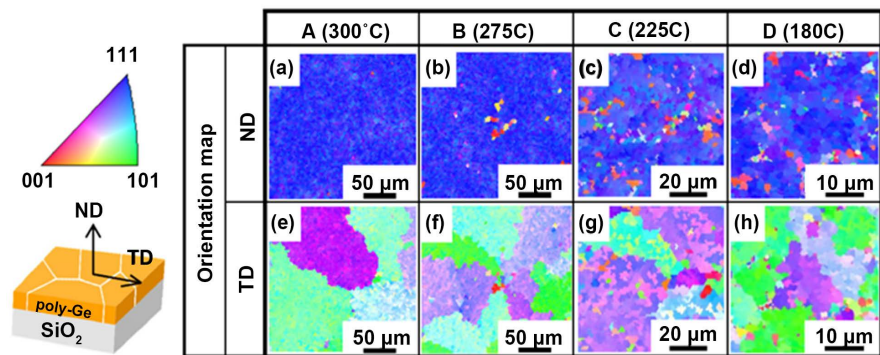


**Figure 8.** EBSD images of poly-Ge for the samples A, B, C and D: (a)-(d) ND and (e)-(h) TD relative to substrate, where the ND and TD figures correspond to the same zone. The other colors indicate the crystal other orientation planes.

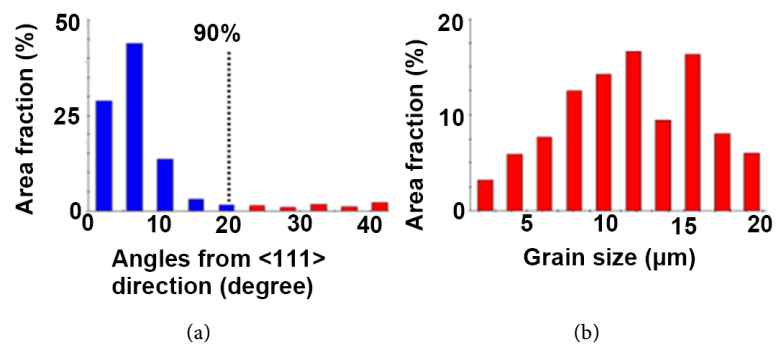


**Figure 9.** Histogram distributions of the (111)-orientation planes ratio (a) and the average grain size (b) of poly-Ge for sample D.

plane from  $0^\circ$  to  $20^\circ$ , and was calculated to be 90%. On the other hand, for the average grain size in **Figure 9(b)**, the average grain size of poly-Ge thin film is  $12\ \mu\text{m}$ . It is worth noting that the (111)-orientation planes ratio is more than 90% and the average grain size is as large as  $12\ \mu\text{m}$  for thin film D crystallized at  $180^\circ\text{C}$  in our second experiments. Therefore, Al induced crystallization enables the larger grain and (111)-orientation planes and lower temperature formation of poly-Ge thin film on  $\text{SiO}_2$  substrate, simultaneously.

#### 4. Conclusion

In summary, the  $T_a$  and  $t_{\text{air}}$  strongly influenced the crystal (111)-orientation planes of a-Ge thin film during Al induce crystallization. The ratio of (111)-orientation planes increases with  $t_{\text{air}}$  increasing and  $T_a$  decreasing. By combining the lower  $T_a$  ( $325^\circ\text{C}$ ) and longer  $t_{\text{air}}$  (30 min), the ratio of (111)-orientation planes reaches over 90%. At the same time, the lower temperature Al induce crystallization of a-Ge thin film can be achieved the larger grain size and (111)-orientation planes of poly-Ge thin film on  $\text{SiO}_2$  substrate. There are mainly two growth promotion techniques: a) The initial Ge atoms are doped in Al thin film by inserting 1 nm thickness a-Ge thin film below Al thin film; b) The diffusion is enhanced by substituting  $\text{GeO}_x$  for  $\text{AlO}_x$  as the diffusion control in-

terlayer. By combining the two techniques, the crystallization temperature can be reduced to 180°C. EBSD measurement proved larger grain size (12  $\mu\text{m}$ ) and higher (111)-orientation plane ratio (>90%) in the resulting Ge thin film on  $\text{SiO}_2$  substrate. The (111)-orientation planes of poly-Ge thin film on  $\text{SiO}_2$  substrate promises to be the higher quality epitaxial layer for developing Ge-based novel flexible photoelectric devices.

## Acknowledgements

This project supported by the National Natural Science Foundation of China (grant No. 11474053) and the innovative entrepreneurial training plan for college students of Guangdong province education department (grant No. XJ2017231).

## References

- [1] Toko, K., Numata, R., Oya, N., Fukata, N., Usami, N. and Suemasu, T. (2014) Low-Temperature (180 °C) Formation of Large-Grained Ge (111) Thin Film on Insulator Using Accelerated Metal-Induced Crystallization. *Applied Physics Letters*, **104**, 022106. <https://doi.org/10.1063/1.4861890>
- [2] Kurosawa, M., Sadoh, T. and Miyao, M. (2014) Comprehensive Study of Al-Induced Layer-Exchange Growth for Orientation-Controlled Si Crystals on  $\text{SiO}_2$  Substrates. *Journal of Applied Physics*, **116**, 173510. <https://doi.org/10.1063/1.4901262>
- [3] Nishimura, T., Lee, C.H., Tabata, T., Wang, S.K., Nagashio, K., Kita, K. and Toriumi, A. (2011) High-Electron-Mobility Ge n-Channel Metal-Oxide-Semiconductor Field-Effect Transistors with High-Pressure Oxidized  $\text{Y}_2\text{O}_3$ . *Applied Physics Express*, **4**, 064201. <https://doi.org/10.1143/APEX.4.064201>
- [4] Kurosawa, M., Toko, K., Kawabata, N., Sadoh, T. and Miyao, M. (2011) Al-Induced Oriented-Crystallization of Si Films on Quartz and Its Application to Epitaxial Template for Ge Growth. *Solid-State Electronics*, **60**, 7-12. <https://doi.org/10.1016/j.sse.2011.01.033>
- [5] Peng, S., Hu, D. and He, D. (2012) Low-Temperature Preparation of Polycrystalline Germanium Thin Films by Al-Induced Crystallization. *Applied Surface Science*, **258**, 6003-6006. <https://doi.org/10.1016/j.apsusc.2012.02.080>
- [6] Kurosawa, M., Kawabata, N., Sadoh, T. and Miyao, M. (2012) Enhanced Interfacial-Nucleation in Al-Induced Crystallization for (111) Oriented  $\text{Si}_{1-x}\text{Ge}_x$  ( $0 \leq x \leq 1$ ) Films on Insulating Substrates. *ECS Journal of Solid State Science and Technology*, **1**, 144-147. <https://doi.org/10.1149/2.010203jss>
- [7] Hu, S., Marshall, A.F. and McIntyre, P.C. (2010) Interface-Controlled Layer Exchange in Metal-Induced Crystallization of Germanium Thin Films. *Applied Physics Letters*, **97**, 082104. <https://doi.org/10.1063/1.3480600>
- [8] Jung, M., Okada, A., Saito, T., Suemasu, T. and Usami, N. (2010) On the Controlling Mechanism of Preferential Orientation of Polycrystalline-Silicon Thin Films Grown by Aluminum-Induced Crystallization. *Applied Physics Express*, **3**, 095803. <https://doi.org/10.1143/APEX.3.095803>
- [9] Kurosawa, M., Kawabata, N., Sadoh, T. and Miyao, M. (2009) Orientation-Controlled Si Thin Films on Insulating Substrates by Al-Induced Crystallization Combined with Interfacial-Oxide Layer modulation. *Applied Physics Letters*, **95**, 132103. <https://doi.org/10.1063/1.3241076>
- [10] Germain, P., Zellama, K., Squelard, S., Bourgoin, J.C. and Gheorghiu, A. (1979)

- Crystallization in Amorphous Germanium. *Journal of Applied Physics*, **50**, 6986. <https://doi.org/10.1063/1.325855>
- [11] Sarikov, A., Schneider, J., Berghold, J., Muske, M., Sieber, I., Gall, S. and Fuhs, W. (2010) A Kinetic Simulation Study of the Mechanisms of Aluminum Induced Layer Exchange Process. *Journal of Applied Physics*, **107**, 114318. <https://doi.org/10.1063/1.3431385>
- [12] Hu, S. and McIntyre, P.C. (2012) Nucleation and Growth Kinetics during Metal-Induced Layer Exchange Crystallization of Ge Thin Films at Low Temperatures. *Journal of Applied Physics*, **111**, 044908. <https://doi.org/10.1063/1.3682110>
- [13] Kurosawa, M., Taoka, N., Sakashita, M., Nakatsuka, O., Miyao, M. and Zaima, S. (2013) Liquid-Sn-Driven Lateral Growth of Poly-GeSn on Insulator Assisted by Surface Oxide Layer. *Applied Physics Letters*, **103**, 101904. <https://doi.org/10.1063/1.4820405>
- [14] Stekolnikov, A.A., Furthmuller, J. and Bechstedt, F. (2002) Absolute Surface Energies of Group-IV Semiconductors: Dependence on Orientation and Reconstruction. *Physical Review B*, **65**, 115318. <https://doi.org/10.1103/PhysRevB.65.115318>
- [15] Toko, K., Kurosawa, M., Saitoh, N., Yoshizawa, N., Usami, N., Miyao, M. and Suemasu, T. (2012) Highly (111)-Oriented Ge Thin Films on Insulators Formed by Al-Induced crystallization. *Applied Physics Letters*, **101**, 072106. <https://doi.org/10.1063/1.4744962>
- [16] Tada, M., Park, J.H., Jain, J.R. and Saraswat, K.C. (2009) Low-Temperature, Low-Pressure Chemical Vapor Deposition and Solid Phase Crystallization of Silicon-Germanium Films. *Journal of the Electrochemical Society*, **156**, D23-D27. <https://doi.org/10.1149/1.3008009>
- [17] Sze, S.M. (1981) *Physics of Semiconductor Devices*. 2nd Edition, Wiley, New York, Chapter 1, 11.
- [18] Fukata, N., Sato, K., Mitome, M., Bando, Y., Sekiguchi, T., Kirkham, M., Hong, J.-I., Wang, Z.L. and Snyder, R.L. (2010) Doping and Raman Characterization of Boron and Phosphorus Atoms in Germanium Nanowires. *ACS Nano*, **4**, 3807-3816. <https://doi.org/10.1021/nn100734e>
- [19] Tsao, C.Y., Weber, J.W., Campbell, P., Widenborg, P.I., Song, D. and Green, M.A. (2009) Low-Temperature Growth of Polycrystalline Ge Thin Film on Glass by *in situ* Deposition and *ex situ* Solid-Phase Crystallization for Photovoltaic Applications. *Applied Surface Science*, **255**, 7028-7035. <https://doi.org/10.1016/j.apsusc.2009.03.035>
- [20] Oya, N., Toko, K., Saitoh, N., Yoshizawa, N. and Suemasu, T. (2014) Direct Synthesis of Highly Textured Ge on Flexible Polyimide Films by Metal-Induced Crystallization. *Applied Physics Letters*, **104**, 262107. <https://doi.org/10.1063/1.4887236>
- [21] Park, J.H., Suzuki, T., Kurosawa, M., Miyao, M. and Sadoh, T. (2013) Nucleation-Controlled Gold-Induced-Crystallization for Selective Formation of Ge(100) and (111) on Insulator at Low-Temperature (~250 °C). *Applied Physics Letters*, **103**, 082102. <https://doi.org/10.1063/1.4819015>